Coalescence of magnetic flux ropes in the ion diffusion region of magnetic reconnection

Rongsheng Wang^{1,2*}, Quanming Lu^{2*}, Rumi Nakamura³, Can Huang², Aimin Du¹, Fan Guo⁴, Waileong Teh⁵, Mingyu Wu², San Lu² and Shui Wang²

Magnetic reconnection is an important process in space1-5 and laboratory⁶ plasmas that effectively converts magnetic energy into plasma kinetic energy within a current sheet. Theoretical work⁷ suggested that reconnection occurs through the growth and overlap of magnetic flux ropes that deconstruct magnetic surfaces in the current sheet and enable the diffusion of the magnetic field lines between two sides of the sheet. This scenario was also proposed as a primary mechanism for accelerating energetic particles during reconnection⁸, but experimental evidence has remained elusive. Here, we identify a total of 19 flux ropes during reconnection in the magnetotail. We found that the majority of the ropes are embedded in the Hall magnetic field region and 63% of them are coalescing. These observations show that the diffusion region is filled with flux ropes and that their interaction is intrinsic to the reconnection dynamics, leading to turbulence.

Magnetic flux ropes (also called plasmoids or current filaments) are localized helical magnetic structures⁹⁻¹¹ and are commonly immersed in reconnection outflow^{12,13}. Recent numerical simulations suggested that plasmoid instability takes place both in the Sweet–Parker current sheet for a large Lundquist number^{14–17} and in elongated electron-scale current layers^{17–20}. Moreover, the interaction of these plasmoids results in fast reconnection and energizes electrons^{18,19}. However, the coalescence by which a pair of flux ropes merges into a larger one^{21–23}, has not yet been confirmed directly by *in situ* observations, although remote observations have been reported^{24,25}. Here, we present the first *in situ* detection of flux rope coalescence during reconnection. The observations established that coalescence is prevalent and plays a crucial role in energy dissipation during reconnection.

A reconnection with a guide field ($B_g \approx -10 \text{ nT}$) was retreating tailwards on 17 August 2003 at $-17R_E$ in the magnetotail. The ion diffusion region, marked with the green bar at the top of Fig. 1, has already been identified on the basis of the coincident reversals of the high-speed flows V_L (Fig. 1a) and B_N (Fig. 1b), and the distorted Hall quadrupolar structure in the local current system (*LMN*; ref. 26). At this time, magnetic field data sampled at 1/67 s were available and the spacecraft separation was smaller than 200 km, so the fine structure within the ion diffusion region could be investigated further.

The spacecraft traversed the reconnection region mainly in the Southern Hemisphere with several excursions into the Northern Hemisphere (Fig. 1b). The magnetic field fluctuated strongly inside the ion diffusion region. Examining the fluctuations, a large number of localized helical magnetic structures were identified and characterized by a distinctly bipolar B_N signature with a sign change and a significant $B_M - B_g$ enhancement near the B_N reversal point (Fig. 1c,d). This type of magnetic structure is generally interpreted as a magnetic flux rope9-13. We focused on only the ropes that were simultaneously detected by all four satellites, and a total of 19 ropes were identified (see Supplementary Table) and colour-coded in Fig. 1b. Each pale blue bar denotes a single rope whereas each pink bar encompasses a pair of ropes later confirmed to be coalescing. For illustrative purposes, the ropes during 16:32–16:46 UT including all the coalescences tailwards of the X-line are expanded in Fig. 1c,d. Most of the ropes are identified only with the data in high resolution (red curve), for example, the ropes marked with arrows above Fig. 1c, which are enlarged in Fig. 3a-c. By using the data sampled at 0.25 s⁻¹ (black curve), only one rope could be discerned at 16:40:47 UT marked with an asterisk in Fig. 1c, whereas another bipolar signature appeared in the trailing part when the data sampled at 67 s⁻¹ was used (red curve). The two ropes are further explored in Fig. 2 to confirm the coalescence.

If a pairwise rope was coalescing, to fulfil energy dissipation the coalescence electric field and current should be induced in their interaction region. In the case of Earth's magnetotail, both the induced coalescence electric field and current would point to the dawn-side²¹⁻²³. The two ropes mentioned above were observed with a strong core field down to -40 nT (Fig. 2c) near the centres at 16:40:47 and 16:41:15 UT (the vertical black lines) in Fig. 2a-f. The electron density (Fig. 2a) and temperature (white line in Fig. 2f) also increased. The interaction region is shaded in pink in Fig. 2b and enlarged in Fig. 2g-k. At ~16:41:11.6 UT (the vertical pink line), a narrow current layer directed to the dawn-side is measured $(j_M \approx -40 \text{ nA m}^{-2}, \text{Fig. 2j})$. An apparent asymmetric distribution of B_N and N_e between two sides of the current layer is measured. B_N $(N_{\rm e})$ evolves from $-20 (1.6 \,{\rm cm}^{-3})$ on the left to $10 \,{\rm nT} (1.1 \,{\rm cm}^{-3})$ on the right. Using the Timing method, we estimate the velocities v_L of the ropes at 16:40:47 and 16:41:15 UT to be -375 and -629 km s⁻¹, respectively. Namely, the rope at 16:41:15 UT is colliding with the one ahead of it (Fig. 4a), which could be the reason for the asymmetric distribution of B_N and N_e . The duration of the current layer is about 0.3 s, and therefore the spatial scale of the layer is evaluated to be $0.3 \,\mathrm{s} \times 375 \,\mathrm{km} \,\mathrm{s}^{-1} \sim 6.6 d_{\mathrm{e}}$ (d_{e} : electron inertial length for $N_{\rm e} = 0.1 \, {\rm cm}^{-3}$) in the L direction. This current layer is expected to be the dissipation region of coalescence.

The electric field in the rest frame of the layer can be estimated by $E_M' = E_M + (\mathbf{V} \times \mathbf{B})_M$. The velocity (**V**) is primarily in the *L* direction

¹Key Laboratory of Earth and Planetary Physics, Institute of Geology and Geophysics, Chinese Academy of Sciences, Beijing 100029, China. ²CAS Key Laboratory of Geospace Environment, Department of Geophysics and Planetary Science, University of Science and Technology of China, Hefei 230026, China. ³Space Research Institute, Austrian Academy of Sciences, Graz 8042, Austria. ⁴Los Alamos National Laboratory, PO Box 1663, Los Alamos, New Mexico 87545, USA. ⁵Space Science Centre (ANGKASA), Universiti Kebangsaan Malaysia, Bangi, Selangor 43600, Malaysia. ^{*}e-mail: rswan@ustc.edu.cn; gmlu@ustc.edu.cn



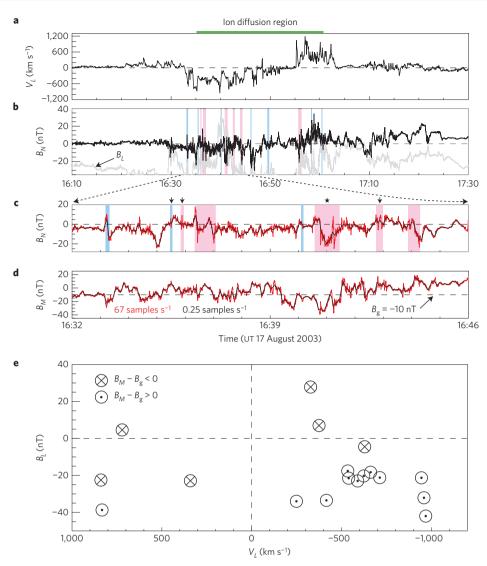


Figure 1 | **Overview of magnetic reconnection and magnetic flux ropes.** The data is presented in the *LMN* coordinates determined by applying minimum variance analysis to the magnetic field data during the 15:50-16:20 UT interval on 17 August 2003 when the current sheet was quiet, to avoid the influence of the Hall current system inside the ion diffusion region, L = (0.957, 0.237, -0.166), M = (-0.271, 0.935, -0.228), and N = (0.102, 0.263, 0.959) relative to the GSM coordinates. The *M* component is primarily along the dawn-dusk direction. **a**, The bulk flows in the *L* direction, available only at C4. **b**, *N* (black curve) and *L* (grey curve) components of the magnetic field at C2. Blue shading indicates single ropes, pink represents pairs of coalescing ropes. **c,d**, *B*_N and *B*_M sampled at 67 s⁻¹ (red curve) and 0.25 s⁻¹ (black curve) from 16:32 to 16:46 UT. The asterisk above panel **c** indicates the ropes expanded in Fig. 2 whereas the three arrows correspond to the ropes shown in Fig. 3a-c. **e**, Each circle corresponds to one rope in the ion diffusion region. Its position is determined by the average values of *V*_L and *B*_L of the rope. The velocity *V*_L is estimated by the time delay between C2 and C3, which are widely separated in the *L* direction and close to each other in the other two directions

and B_N is close to 0 at the B_N reversal point, so $E_M' \approx E_M$ around this point. The electric field was only measured in the Cluster spin plane (x-y) of the Inverted Spin Reference system. The *y* component is (0, 0.948, -0.319) in the GSM coordinates and primarily in the M direction, so E_{ν} is close to $E_M(E_M \approx E_{\nu})$ around the point. E_{ν} displays a localized minimum value (-2.8 mV m^{-1}) near the B_N reversal point (Fig. 2i). The polarities of j_M and E_M fit the expected coalescence current and electric field. Therefore, we conclude that the ropes were coalescing. $j_M E_M' > 0$ indicates that magnetic energy was released. The core field of the ropes is two times larger than the coalescing field (Fig. 2g) and is presumably the coalescence guide field. Thus, this coalescence is intrinsically an asymmetric component reconnection. In the surrounding of the current layer, the current j_N significantly increases and points south, its width estimated to be 0.8 d_i ($d_i \approx 720$ km). The negative j_N could be explained by the coalescence outflow.

In the same way, five more coalescences could be identified. The coalescences in the tailward flow at ~16:35:49 and ~16:42:45 UT and in the earthward flow at 16:55:47 UT are shown in Fig. 3b,c and Fig. 3d, respectively. At the coalescing points, j_M and E_y are negative, that is pointing dawn-side. Occasionally, the spacecraft repeatedly crossed one coalescence dissipation region (Fig. 3d). Figure 3e,f show the superposed epoch analysis of E_y and j_M in the 6 coalescences and the time domain is ± 3 s. The minimum value of $E_y(j_M)$ was taken as the zero epoch in Fig. 3e (Fig. 3f). On average, the energy dissipation rate of these coalescences is about 200 pw m⁻³, much higher than that (45 pw m⁻³) of the usual reconnection in the magnetotail²⁷. Using Faraday's law ($\Delta E_y \sim 10$ mV m⁻¹, $\Delta L \sim 100$ km, $\Delta B_N \sim 10$ nT), we estimate the dynamic timescale of the coalescence to be 0.1 τ_A (Alfvenic time $\tau_A \approx 1$ s).

Various ropes in the ion diffusion region have a core field opposite to the guide field (Fig. 1c,d and Supplementary

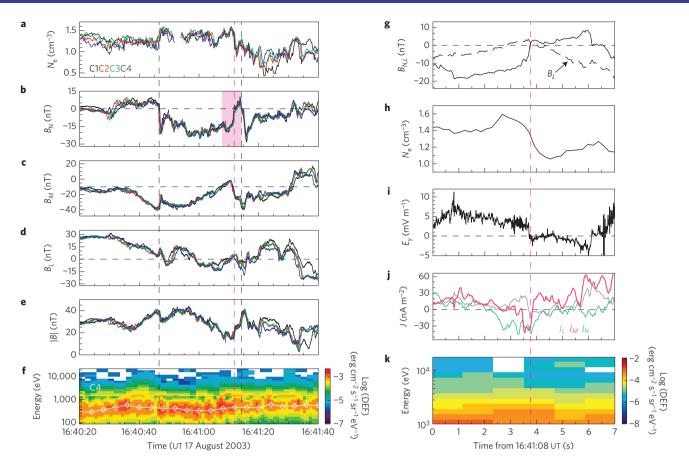


Figure 2 | An example of coalescence. **a**, Electron density derived from the spacecraft potential. **b**-**e**, $N(\mathbf{b})$, $M(\mathbf{c})$, $L(\mathbf{d})$ components and magnitude (**e**) of the magnetic field at all four satellites. **f**, Electron differential energy fluxes (DEFs) at C4, the white line is the electron temperature. The vertical black dashed lines at ~16:40:47 and ~16:41:15 UT correspond to the centres of the ropes and the pink dashed line signifies the coalescing point. The pink bar in **b** represents the interaction region between the two ropes. Measurements in the interaction region at C4 were enlarged in **g**-**k**. **g**, B_N and B_L . **h**, Electron density. **i**, Electric field E_y in the inverted spin reference system. **j**, Three components of the current density. **k**, Electron differential energy fluxes from the sensor HEEA of the PEACE instrument.

Information), for example, the ropes in Fig. 3a,c were detected at $B_L < -25$ nT and the core field was larger than 10 nT. The peaks of the core field B_M and current j_M indicate that the spacecraft crossed the rope centres. The sign discrepancy between the core field and the guide field implies that the guide field was not the unique source for the core field. A scatterplot of the average v_L and B_L at C2 of these ropes is shown in Fig. 1e. The negative core field (circles with a cross) predominantly appears in the upper right and lower left quadrants whereas the positive core field (circles with a dot) is mainly found in the lower right quadrant, which is consistent with the distorted Hall quadrupolar structure²⁶. Therefore, this indicates that the core field is generated by the compression of the ambient Hall field. In other words, the majority of the ropes are situated in the region of the Hall field rather than centred in the plasma sheet. This conclusion is in agreement with prior observations²⁸. Consequently, a new scenario for the diffusion region is illustrated in Fig. 4b. The colour-coded ellipses along the trajectory represent the ropes marked in the same colour in Fig. 1b.

During this reconnection event, the thin current layers near the neutral plane and the separatrices were found to expand to tens of the ion inertial length in the *L* direction²⁶. Thus, the identified ropes could only result from the breakup of the current layers, as suggested by simulations^{14–19} and only verified in the laboratory²⁹. After the ropes are formed, they coalesce and give rise to small diffusion regions on the electron scale. Namely, the small diffusion region. The observations show a clear turbulent energy cascade.

Recent simulations¹⁹ suggested that reconnection is dominated by the formation and interaction of magnetic flux ropes, the majority of which are generated by the instabilities of the electron current layers along the separatrices, and evolves into turbulence. This picture is consistent with our observations. However, a further quantitative comparison between the observations and simulations is needed.

Received 15 May 2012; accepted 29 October 2015; published online 7 December 2015

References

- Dungey, J. W. Interplanetary magnetic field and auroral zones. *Phys. Rev. Lett.* 6, 47–48 (1961).
- Paschmann, G. et al. Plasma acceleration at the Earths magnetopause—evidence for reconnection. Nature 282, 243–246 (1979).
- Angelopoulos, V. et al. Tail reconnection triggering substorm onset. Science 321, 931–935 (2008).
- Kronberg, P. P. Intergalactic magnetic fields. *Phys. Today* 55, 40–46 (December, 2002).
- Hurley, K. et al. An exceptionally bright flare from SGR 1806–20 and the origins of short-duration gamma-ray bursts. *Nature* 434, 1098–1103 (2005).
- Yamada, M. *et al.* Investigation of magnetic reconnection during a Sawtooth crash in a high-temperature Tokamak plasma. *Phys. Plasmas* 1, 3269–3276 (1994).
- Galeev, A. A., Kuznetsova, M. M. & Zeleny, L. M. Magnetopause stability threshold for Patchy reconnection. *Space Sci. Rev.* 44, 1–41 (1986).
- Drake, J. F., Swisdak, M., Che, H. & Shay, M. A. Electron acceleration from contracting magnetic islands during reconnection. *Nature* 443, 553–556 (2006).
- Russell, C. T. & Elphic, R. C. Initial Isee magnetometer results—magnetopause observations. Space Sci. Rev. 22, 681–715 (1978).

LETTERS

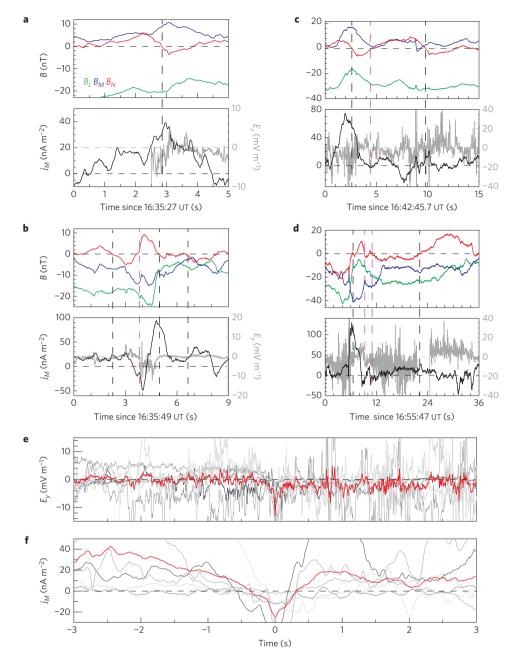


Figure 3 | Average properties of coalescence. **a**-**d**, The data is shown in the same format in plots **a**-**d**: B_L (green), B_M (blue) and B_N (red) are displayed in the first panel, and the current density j_M as well as the electric field E_y are shown in the second panel. The vertical black dashed lines correspond to the rope centre and the pink dashed lines represent the merging points. The electric field E_y variation is strong within the ropes but is negative near the coalescing point. **e**,**f**, A superposed epoch analysis of E_y (**e**) and j_M (**f**) in the interaction regions of 6 coalescences (grey lines) identified inside the ion diffusion region. The electric field data at C4 was used.

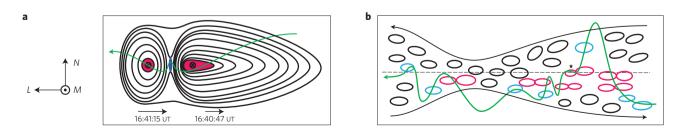


Figure 4 | **Schematics for the coalescence and the ion diffusion region. a**, A pairwise flux rope coalescence, corresponding to the coalescing ropes with an asterisk in Figs 1c and 2 and **b**. The ellipses in red (blue) indicate that the current density is positive (negative) along the *M* direction. The green curve denotes the spacecraft trajectory. **b**, A new scenario for the ion diffusion region of collisionless reconnection in the magnetotail. The colour-coded ellipses represent the flux ropes detected by the spacecraft in the ion diffusion region. The pink ellipses denote the coalescing ropes.

NATURE PHYSICS DOI: 10.1038/NPHYS3578

- Sibeck, D. G. *et al.* Magnetotail flux ropes. *Geophys. Res. Lett.* 11, 1090–1093 (1984).
- Moldwin, M. B. & Hughes, W. J. Plasmoids as magnetic-flux ropes. J. Geophys. Res. 96, 14051–14064 (1991).
- 12. Slavin, J. A. *et al.* Geotail observations of magnetic flux ropes in the plasma sheet. *J. Geophys. Res.* **108**, 1015 (2003).
- Chen, L. J. et al. Observation of energetic electrons within magnetic islands. Nature Phys. 4, 19–23 (2008).
- Lapenta, G. Self-feeding turbulent magnetic reconnection on macroscopic scales. *Phys. Rev. Lett.* 100, 235001 (2008).
- Bhattacharjee, A., Huang, Y. M., Yang, H. & Rogers, B. Fast reconnection in high-Lundquist-number plasmas due to the plasmoid instability. *Phys. Plasmas* 16, 112102 (2009).
- Samtaney, R., Loureiro, N. F., Uzdensky, D. A., Schekochihin, A. A. & Cowley, S. C. Formation of plasmoid chains in magnetic reconnection. *Phys. Rev. Lett.* **103**, 105004 (2009).
- 17. Daughton, W. *et al.* Transition from collisional to kinetic regimes in large-scale reconnection layers. *Phys. Rev. Lett.* **103**, 065004 (2009).
- Drake, J. F., Swisdak, M., Schoeffler, K. M., Rogers, B. N. & Kobayashi, S. Formation of secondary islands during magnetic reconnection. *Geophys. Res. Lett.* 33, L13105 (2006).
- Daughton, W. *et al.* Role of electron physics in the development of turbulent magnetic reconnection in collisionless plasmas. *Nature Phys.* 7, 539–542 (2011).
- Guo, F., Li, H., Daughton, W. & Liu, Y. H. Formation of Hard Power Laws in the energetic particle spectra resulting from relativistic magnetic reconnection. *Phys. Rev. Lett.* **113**, 155005 (2014).
- Dorelli, J. C. & Birn, J. Whistler-mediated magnetic reconnection in large systems: Magnetic flux pileup and the formation of thin current sheets. *J. Geophys. Res.* 108, 1133 (2003).
- Pritchett, P. L. Kinetic properties of magnetic merging in the coalescence process. *Phys. Plasmas* 14, 052102 (2007).
- Oka, M., Phan, T. D., Krucker, S., Fujimoto, M. & Shinohara, I. Electron acceleration by multi-island coalescence. *Astrophys. J.* 714, 915–926 (2010).
- Song, H. Q., Chen, Y., Li, G., Kong, X. L. & Feng, S. W. Coalescence of macroscopic magnetic islands and electron acceleration from STEREO observation. *Phys. Rev. X* 2, 021015 (2012).

- Gopalswamy, N., Yashiro, S., Kaiser, M. L., Howard, R. A. & Bougeret, J. L. Interplanetary radio emission due to interaction between two coronal mass ejections. *Geophys. Res. Lett.* 29, 106-1–106-4 (2002).
- Wang, R. S. *et al.* Observation of multiple sub-cavities adjacent to single separatrix. *Geophys. Res. Lett.* 40, 2511–2517 (2013).
- 27. Zenitani, S., Shinohara, I. & Nagai, T. Evidence for the dissipation region in magnetotail reconnection. *Geophys. Res. Lett.* **39**, L11102 (2012).
- Eastwood, J. P. *et al.* Multi-point observations of the Hall electromagnetic field and secondary island formation during magnetic reconnection. *J. Geophys. Res.* 112, A06235 (2007).
- 29. Dorfman, S. *et al.* Three-dimensional, impulsive magnetic reconnection in a laboratory plasma. *Geophys. Res. Lett.* **40**, 233–238 (2012).

Acknowledgements

R.W. appreciates the valuable suggestions from W. Daughton at Los Alamos National Laboratory. All Cluster data other than the PEACE data are available at Cluster Science Archive (http://www.cosmos.esa.int/web/csa). We thank the FGM, CIS, EFW, PEACE, and RAPID instrument teams. This work is supported by the National Science Foundation of China (NSFC; grants 41474126, 41331067, 41174122, 11220101002 and 41104092) and by the National Basic Research Program of China (2014CB845903 and 2013CBA01503). This work at Austria is supported by the Austrian Science Fund (FWF) I429-N16.

Author contributions

R.W. carried out data analysis, interpreted the results, and wrote the paper. Q.L. provided the theoretical analysis. Q.L., C.H., R.N., F.G., W.T., A.D. and S.W. participated in discussion and interpretation of the data. F.G. and Q.L. improved language of the manuscript. M.W. and S.L. participated in the earlier discussion. All of the authors made significant contributions to this work.

Additional information

Supplementary information is available in the online version of the paper. Reprints and permissions information is available online at www.nature.com/reprints. Correspondence and requests for materials should be addressed to R.W. or Q.L.

Competing financial interests

The authors declare no competing financial interests.